

1

# INGRID Analysis Technical Note

2

Masashi Otani

3

Akira Murakami

4

Christophe Bronner

5

for INGRID group

6

December 28, 2010

### Abstract

8 In this note we summarize the INGRID analysis results with 2010a data. We  
9 measured the neutrino event rate, the beam profile center and these stability  
10 for the confirmation and support of 2010a oscillation analysis. We select the  
11 neutrino interaction, mainly charged current interaction, at each module and  
12 reconstruct the neutrino beam profile. We compare some distributions between  
13 data and MC and found good agreement. We get the data/MC ratio for the  
14 event rate to be  $1.074 \pm 0.001(\text{stat.}) \pm 0.040(\text{syst.})$ . The center of the neutrino  
15 beam profile found to be  $0.2 \pm 1.4(\text{stat.}) \pm 9.2(\text{syst.})$  cm for X profile and  
16  $-6.6 \pm 1.5(\text{stat.}) \pm 10.4(\text{syst.})$  cm for Y profile. Finally the off-axis angle is  
17 measured to be 2.52 degrees with the error of 0.37 mrad.

# Contents

19	<b>1</b>	<b>Introduction</b>	<b>3</b>
20	<b>2</b>	<b>Monte Carlo simulation</b>	<b>5</b>
21	<b>3</b>	<b>Neutrino event selection</b>	<b>10</b>
22	3.1	Event selection . . . . .	10
23	3.2	Basic distribution of data and MC simulation . . . . .	15
24	3.3	Reconstruction resolution . . . . .	17
25	3.4	Efficiency to neutrino interaction . . . . .	18
26	<b>4</b>	<b>Event rate measurements</b>	<b>20</b>
27	4.1	Data set . . . . .	20
28	4.2	Event rate stability . . . . .	20
29	4.3	The data/MC ratio . . . . .	21
30	4.4	Systematic error of event rate . . . . .	26
31	<b>5</b>	<b>Measurements of beam profile</b>	<b>30</b>
32	5.1	Stability of beam center . . . . .	30
33	5.2	The systematic error of beam center . . . . .	31
34	<b>6</b>	<b>Measurement of beam direction</b>	<b>32</b>
35	<b>7</b>	<b>Conclusion</b>	<b>34</b>

# Chapter 1

## Introduction

INGRID is on-axis near detector which consists of identical 14 modules<sup>1</sup> to monitor the beam stability. Each module has a sandwich structure made of the iron plates and the scintillator trackers. INGRID module consists 11 tracking planes which consists 2 layers. Each layer has 24 scintillator bars and the direction of scintillator is perpendicular each other layer.

We count the number of neutrino interactions, mainly CC interaction, occurred inside the module. Based on the number of selected events for each module, the beam profile is reconstructed. Fig.1.1 shows a typical event in an INGRID module. Detector coordinates are shown in Fig.1.2. INGRID uses a right-handed Cartesian coordinate system in which the z axis is the beam direction and the y axis is the vertical upward direction. With this definition the INGRID module number is decided from horizontal modules.

In this note, we describe the measurements of

- (1) neutrino event rate and its stability
- (2) neutrino beam center and its stability
- (3) neutrino beam direction

for the data taken from January to June 2010 (2010a data set).

This article is organized as follows. Chapter 2 explains the overview of Monte Carlo simulation. Chapter 3 explains the neutrino event selection. Finally the result of the event rate measurement, beam profile measurement and beam direction are shown in Chap. 4, Chap. 5 and Chap. 6, respectively.

---

<sup>1</sup>Additional two off-center modules and a proton module are installed after 2010a data taking.

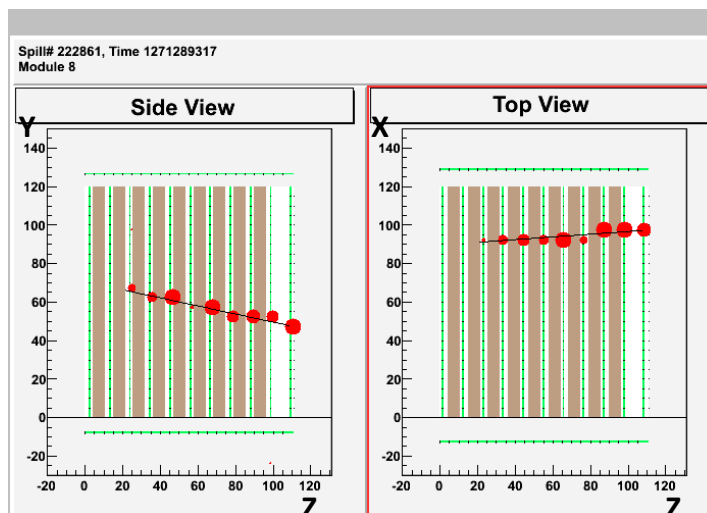


Figure 1.1: The typical neutrino event

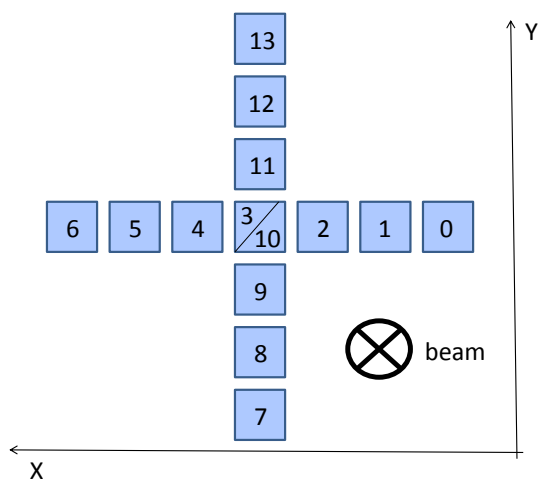


Figure 1.2: INGRID coordinates and the definition of the number of an INGRID module

## Chapter 2

# Monte Carlo simulation

We use three MC simulation programs : jnubeam, NEUT and detector simulation (Fig.2.1).

- Neutrino flux : jubeam (version 10d tuned ver. 2)
- Neutrino interaction to the target : NEUT (version 5.0.6.)
- Detector response simulation based on GEANT4 <sup>1</sup>

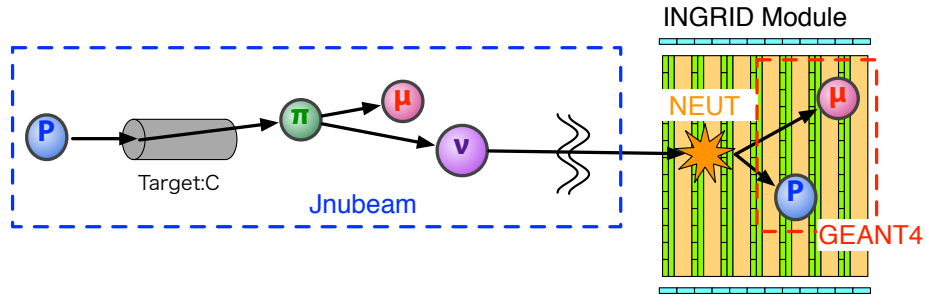


Figure 2.1: INGRID MC overview

### Neutrino flux prediction

Predictions for the neutrino flux are obtained via jnubeam version 10d. For a detailed description of jnubeam, see Ref.[1]. Figure 2.2 shows the neutrino energy spectrum at the INGRID detector location. A total neutrino flux per proton on target of  $5.94 \cdot 10^{-7} \text{ cm}^{-2}$  is expected at the INGRID center module and the flux is dominated by muon neutrinos (95%). Figure 2.3 and Fig.2.4 show

<sup>1</sup>This INGRID MC is not the software of ND280 software packages

the energy spectrum at the INGRID center module and horizontal edge module, and the Super-Kamiokande detector, respectively. Because each INGRID module covers the different off-axis angle, the neutrino energy spectrum is slightly different at each module. Table 2.1 shows the average neutrino energy at each module and the average energy is different for about 0.2 GeV between the center module and the edge module.

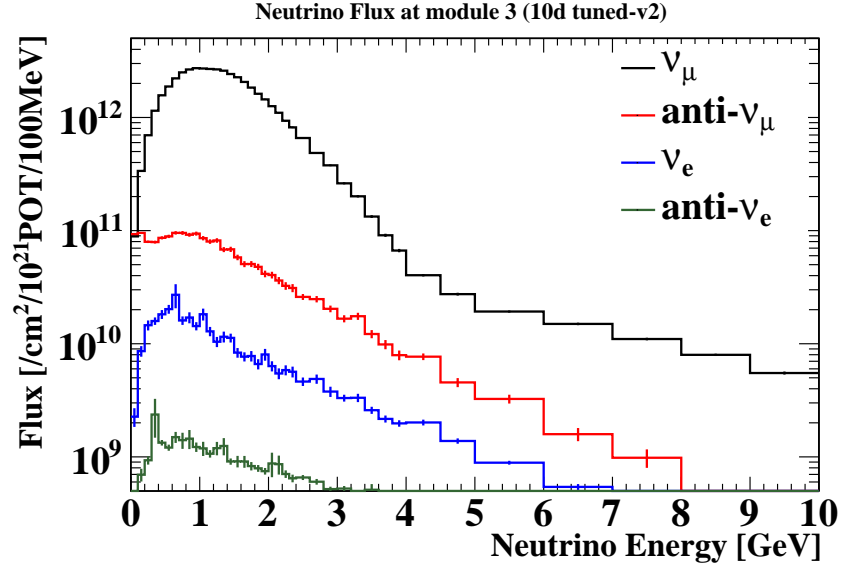


Figure 2.2: Neutrino energy spectrum predicted by jnubeam at the INGRID detector location

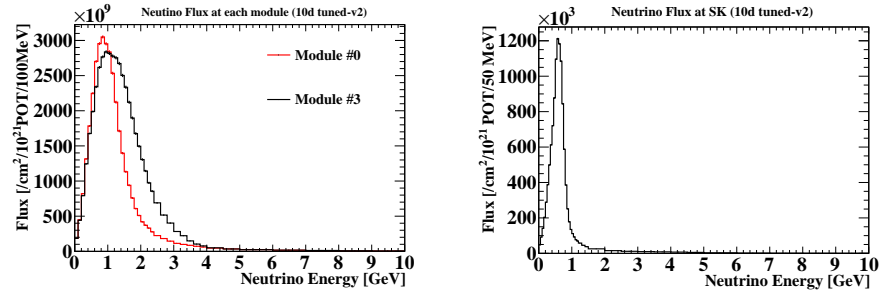


Figure 2.3: Neutrino energy spectrum predicted by jnubeam at the INGRID center module and edge module

Figure 2.4: Neutrino energy spectrum predicted by jnubeam at the SK detector location

module#	0	1	2	3	4	5	6	SK
Average energy[GeV]	1.08	1.20	1.29	1.32	1.29	1.21	1.09	0.61

Table 2.1: Average neutrino energy

## Neutrino interaction simulation

We simulate neutrino interactions with target iron plate (Fe) in the INGRID detector with the NEUT program libraries. Currently, we simulate all the neutrino interaction with iron (Fe) as the target nuclei. Because the fraction of the number of interactions occurred in scintillator and support material is about 4 %, its effect should be small. Simulation with correct material is under preparation. For a detailed description of NEUT, see Ref.[2].

## Detector response simulation

We simulate the detector response to the generated particles from the neutrino interaction with simulator based on GEANT4. We obtain the x and y position of the neutrino interaction from jubeam flux file. The vertex z is uniformly generated in the iron plate and the scintillator tacker taking into account the mass ratio of iron planes (99.54 ton) to scintillator planes (3.74 ton).

Detector response simulation includes following effects which have an impact to the efficiency to the neutrino interactions.

- We tuned the conversion factor from energy deposit to number of photon in MC simulation by adjusting the peak photoelectron (PE) of beam related sand muon. We also include the quenching effect of scintillator, attenuation of photon propagating in the fiber and MPPC response model based on [3]. Figure 2.5 shows the typical PE distribution of beam related sand muon after these MC tuning. The peak PE is well reproduced.
- Although the inefficiency resulted from the photoelectron statistics (light yield is  $\sim 20$  PE at peak and threshold is 2.5 PE) is expected to be less than 0.1%, each channel has 1  $\sim$  2% inefficiency resulted from the gap between scintillator bars, which is studied by cosmic-ray data. In Fig.2.6, black line shows the tracking inefficiency as a function of the angle with respect to z-axis. Because the particle with small angle has more probability to go through the gap, the inefficiency becomes larger for a small angle track. We tuned the cross-section of the scintillator bar in MC with real geometry (Fig.2.7) to reproduce the angular dependence of the inefficiency in data. The blue and red points in Fig.2.6 show the angular dependence of the tracking inefficiency in the MC simulation before and after the tuning, respectively. The angular dependence of the tracking inefficiency is well reproduced in MC.
- Accidental hits by MPPC dark noise result in miss reconstruction of the track and miss identification of the vertex position. As a consequence the



114 selection efficiency is influenced by MPPC dark noise. In MC the MPPC  
 115 noise hit is generated to reproduce the number of PE, timing, and noise  
 116 rate of data. Fig.2.8 shows the timing distribution for data during beam-  
 117 off period and MC. Because the accumulation of the charge due to MPPC  
 118 noise with the ADC less than TDC threshold, the number of hits increase  
 119 with respect to time. The distribution is well reproduced.

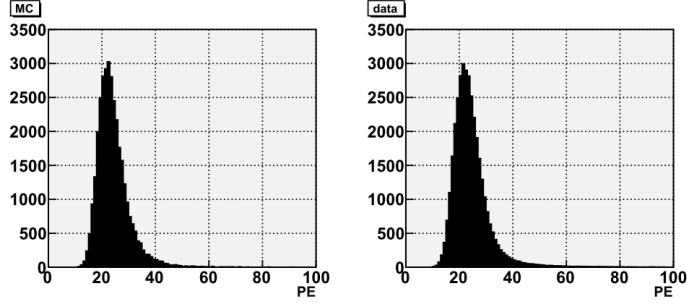


Figure 2.5: PE distribution of beam related sand muon. Left plot is MC simulation and right one is data.

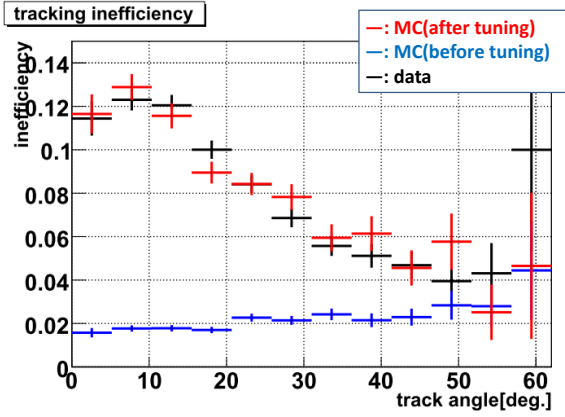


Figure 2.6: Tracking inefficiency as a function of angle of the reconstructed track

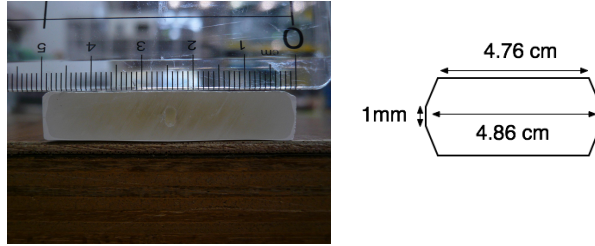


Figure 2.7: Photo of the cross-section of the scintillator bar (left) and the cross-section in MC (right)

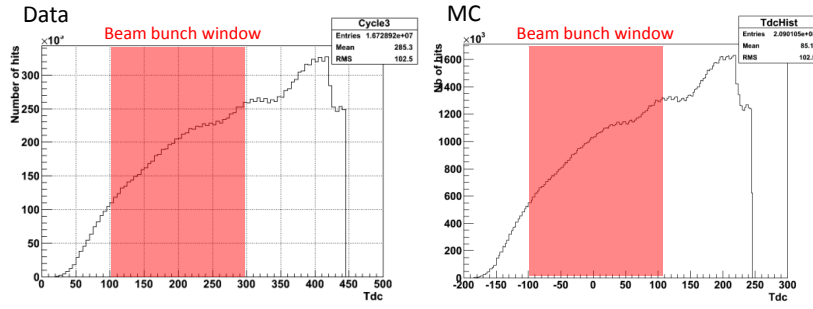


Figure 2.8: The timing distribution of MPPC noise. left is data and right is MC.

## Chapter 3

# Neutrino event selection

### 3.1 Event selection

We select a long track of charged particle started within the fiducial volume of an INGRID module to select the neutrino interaction. In this chapter we use all the beam data shown in Chap.?? and the MC simulation corresponded to an equivalent of  $100 \times 10^{21}$  pot. Before reconstruction of the track, plane activity and PE cut are applied to reject an accidental noise event. After reconstruction of the track, VETO cut and fiducial cut are applied to reject the incoming particle from the neutrino interaction at upstream materials. The order of the event selections is shown below.

- (1) Time clustering
- (2) Number of active planes  $> 2$
- (3)  $\text{PE}/(\text{number of active layers}) > 6.5$
- (4) Tracking
- (5) Track matching
- (6) Beam timing cut
- (7) Upstream VETO cut
- (8) Fiducial volume cut

All the selections are done a module by module and bunch by bunch basis. We explain the detail of each selection below. In this analysis, the channel which has a ADC signal larger than 2.5 PE, which corresponds to TDC threshold, is defined as the hit.

At the first step hits are clustered with following criteria; If there are more than 3 hits within 100 nsec, all the hits within  $\pm 50$  nsec from the average time are brought together into a cluster. Following all the selections are applied

146 to cluster by cluster. Within the cluster the number of planes with at least  
 147 one coincidence hit in both x and y layers, which are called active layers, is  
 148 counted. Figure 3.1 shows the distribution of the number of planes with the  
 149 active layers, which are called active planes. We select the event which has  
 150 more than 2 active planes. Fig.3.2 shows total PE of all hits in the active layer  
 151 divided by the number of active layers ( $\text{PE}/(\text{number of active layers})$ ) after the  
 152 selection with the number of active planes  $> 2$ . The event with more than 6.5  
 153  $\text{PE}/(\text{number of active layers})$  is selected.

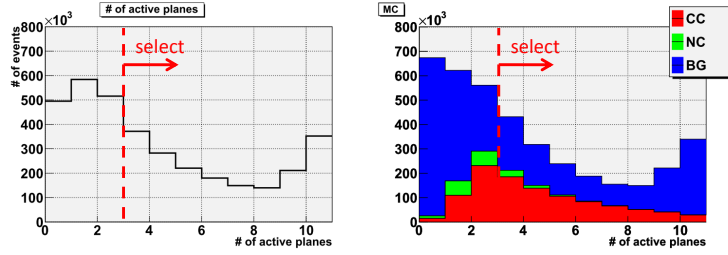


Figure 3.1: The number of active planes(left:DATA, right:MC normalized by area)

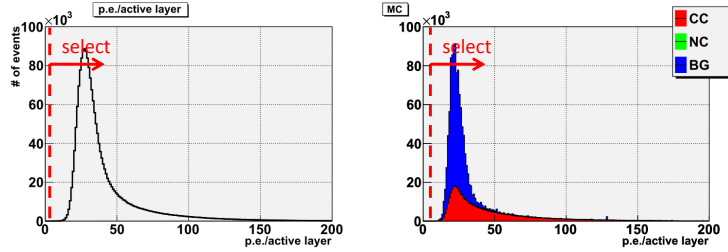


Figure 3.2:  $\text{PE}/(\text{number of active layers})$  after the selection with the number of active planes  $> 2$  (left:DATA, right:MC normalized by area)

154 After these selections track is reconstructed. First the hits in the most  
 155 downstream active x and y layer are adopted as a end-point of the track. Looking  
 156 at the hits in next upstream plane in order, the hit is selected as the track if the  
 157 difference of the slope calculated from the straight line is less than 2 channels.  
 158 Finally the positions of all the selected hits are fitted to a straight line by a least  
 159 square method to get the angle of the reconstructed track. Figure 3.3 shows the

160 angular distribution of the reconstructed track after following track matching  
 161 selection.

162 After reconstruction of the track some badly fitted tracks are rejected by  
 163 considering the difference of the start point  $z$  of a 2-D track in  $x$  view and  $y$   
 164 view. Fig.3.4 shows the distribution of the difference of the start point  $z$  of the  
 165 track between 2-D track in  $x$  view and  $y$  view. We require the difference smaller  
 166 than 2 planes. Because there are some background events such as cosmic-ray  
 167 on beam off timing, the events within  $\pm 100$  nsec from the expected timing of  
 168 each bunch are selected (Fig.3.5).

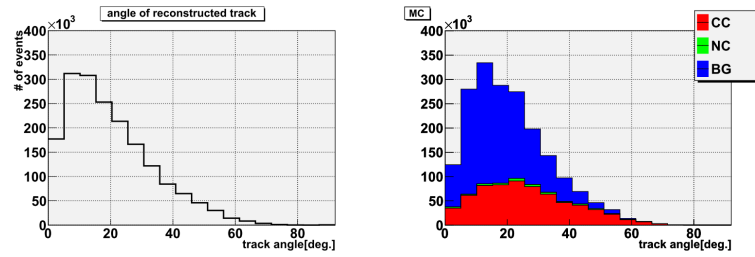


Figure 3.3: Angular distribution of the reconstructed track after all selections after the track matching selection(left:DATA, right:MC normalized by area)

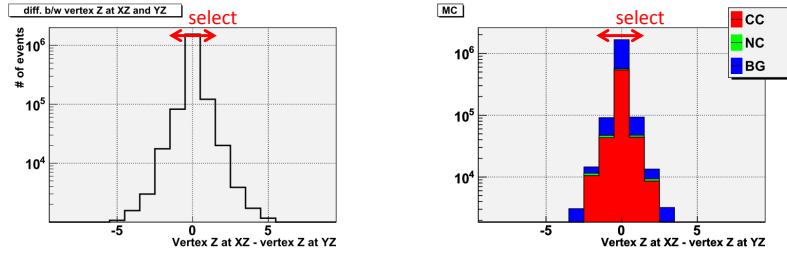


Figure 3.4: Difference of the start point  $z$  of the track in  $x$  view and  $y$  view(left:DATA, right:MC normalized by area)

169 Finally we apply two selections to reject the incoming particles produced by  
 170 the neutrino interaction in upstream materials. First one is upstream VETO  
 171 selection. If the VETO plane has a hit at the upstream position extrapolated  
 172 from the reconstructed track, the event is rejected. Figure 3.6 shows the example  
 173 of the event rejected at this selection. After that we apply fiducial volume cut.

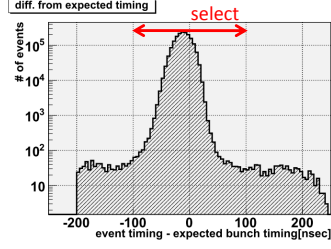


Figure 3.5: Time residual plot after the track matching selection

174 The fiducial volume is the cubic volume which is defined as  $\pm 50 \text{ cm}^2$  transverse  
 175 area from the center of an INGRID module and from 2 to 8-th tracker(Fig.3.7).  
 176 The position of most upstream hit associated with the reconstructed track is  
 177 defined as the vertex and we require that vertex is in the fiducial volume (Fig.3.8  
 and 3.9).

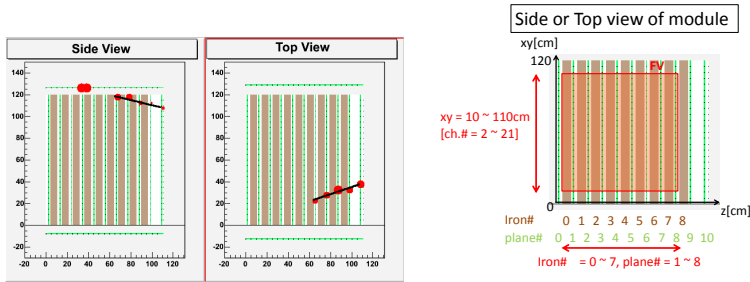


Figure 3.6: The event rejected by upstream VETO selection

Figure 3.7: The definition of fiducial volume

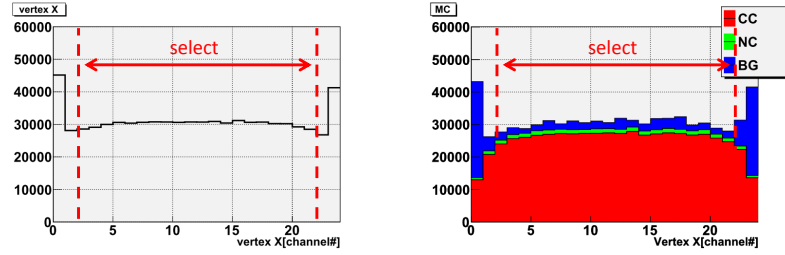


Figure 3.8: vertex x after the upstream VETO cut (left:DATA, right:MC normalized by area)

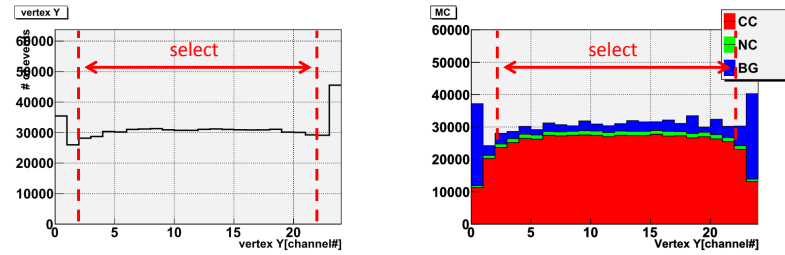


Figure 3.9: vertex y after the upstream VETO cut (left:DATA, right:MC normalized by area)

## 179 Event selection summary

180 The number of events and the selection efficiencies at each selection step is  
 181 summarized in Tab.3.1. We obtained 493813 neutrino event candidates among  
 2010a data set.

	selection	Data	selection eff.	MC	selection eff.
1	# of active planes > 2	1906146		$1.97 \times 10^6$	
2	PE / active layers > 6.5	1906078	(1.00)	$1.97 \times 10^6$	(1.00)
3	Tracking	1804786	(0.95)	$1.83 \times 10^6$	(0.93)
4	Track matching	1749548	(0.97)	$1.77 \times 10^6$	(0.97)
5	Beam timing	1747181	(0.99)	$1.77 \times 10^6$	(1.00)
6	Upstream VETO cut	745912	(0.43)	$7.34 \times 10^5$	(0.42)
7	Vertex in fiducial	493813	(0.66)	$4.73 \times 10^5$	(0.66)

Table 3.1: Summary of the event selection. Data and MC are normalized by pot

182

## 183 3.2 Basic distribution of data and MC simula- 184 tion

185 In this section we show some distributions of the selected events. In each distri-  
 186 bution, there are two plots; one is data and MC simulation overlaid and one is  
 187 data/MC. In each plot the distribution of MC simulation is normalized by the  
 188 area of the distribution of data. The data/MC ratio is within few percents at  
 189 each plot and we found good agreement between DATA and MC.

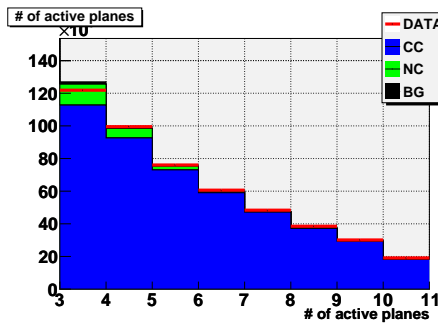


Figure 3.10: number of active planes

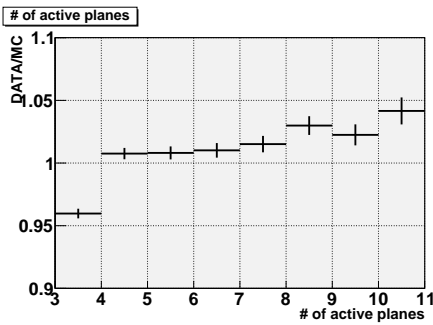


Figure 3.11: DATA/MC



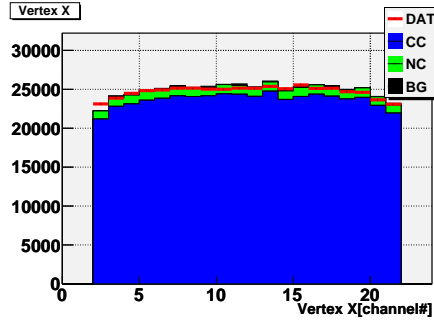


Figure 3.12: Vertex X

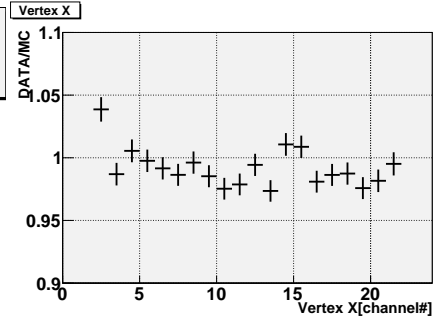


Figure 3.13: DATA/MC

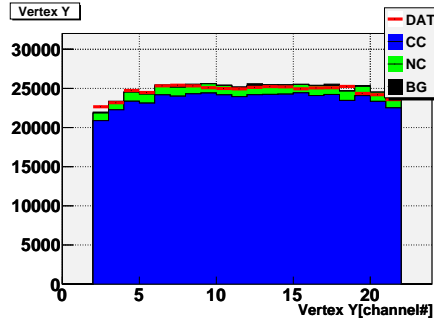


Figure 3.14: Vertex Y

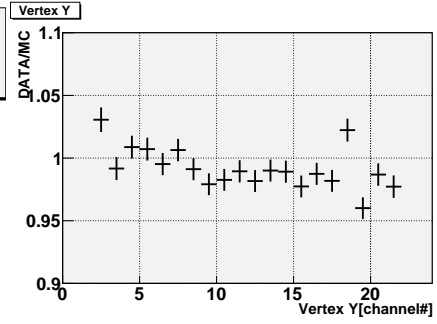


Figure 3.15: DATA/MC

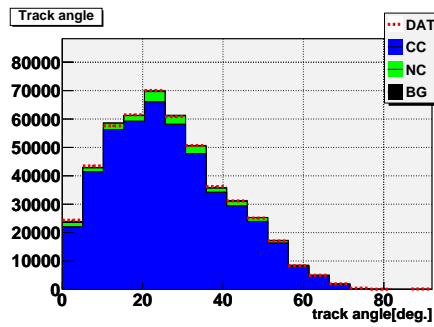


Figure 3.16: Reconstructed track angle

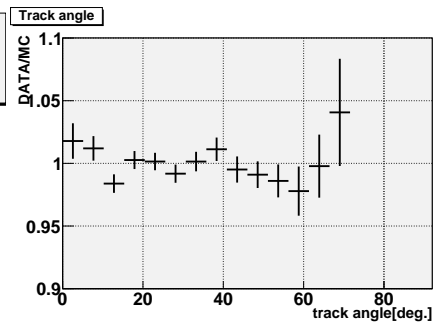


Figure 3.17: DATA/MC

### 3.3 Reconstruction resolution

Reconstruction resolution is checked by MC simulation to compare the reconstructed value and the MC true information. The results of vertex X, Y and track angle are shown in Fig.3.18, Fig.3.19 and 3.20, respectively. Their r.m.s. for CCQE events are 2.7 cm for X, 2.8 cm for Y and 3.8 degree, respectively.

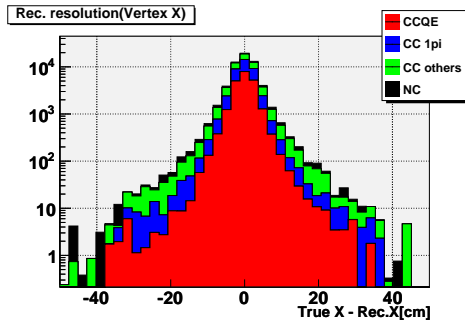


Figure 3.18: X resolution

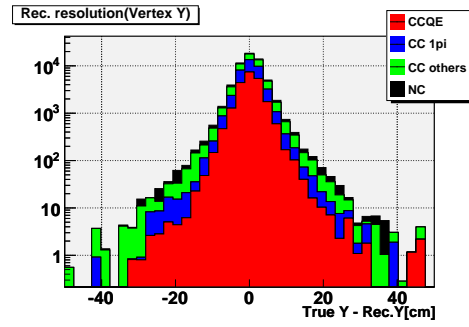


Figure 3.19: Y resolution

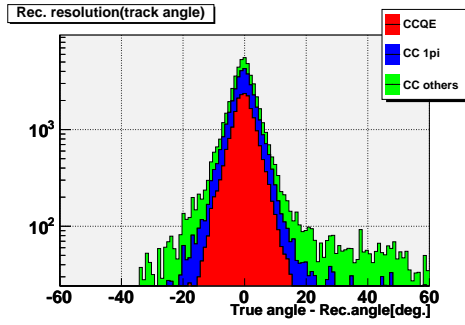


Figure 3.20: Angular resolution of reconstructed track

### 3.4 Efficiency to neutrino interaction

The event selection efficiency as a function of true neutrino energy is shown in Fig.3.21 and 3.22. Here, the efficiency is defined as the ratio of the number of selected events to that of the events generated inside the fiducial volume. Figure 3.23 shows the selection efficiency for CC interactions as a function of the muon angle. Because the acceptance for the muon angle and the muon angle dependence to the neutrino energy (Fig.3.24), the efficiency for CC interaction depends on the neutrino energy. Figure 3.25 shows the efficiency for the muons with all angle and less than 15 degrees. The selection efficiency for the muon with low angle is almost 100% and the rising edge around 0.3 GeV corresponds to the minimum energy of the muon to penetrate the 2 iron plates and 3 scintillator trackers.

Table 3.2 shows the selection efficiency for each module. Because the energy spectrum of the beam neutrino is slightly different module by module, the selection efficiency is also different.

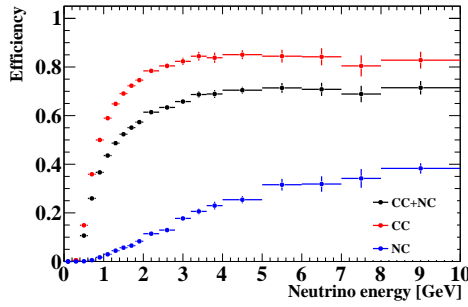


Figure 3.21: Neutrino event selection efficiency

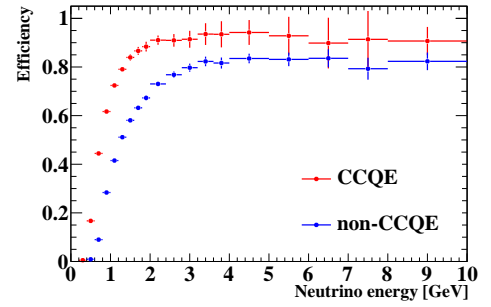


Figure 3.22: Selection efficiency for CCQE and CC others.

module	Efficiency[%]
0	51.7
1	54.0
2	55.1
3	55.1
4	55.0
5	54.2
6	51.2

Table 3.2: Efficiency of each module

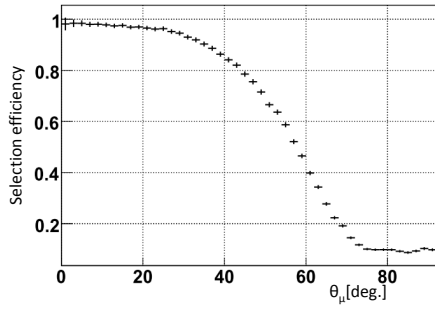


Figure 3.23: The selection efficiency for CC interactions as a function of the muon angle.

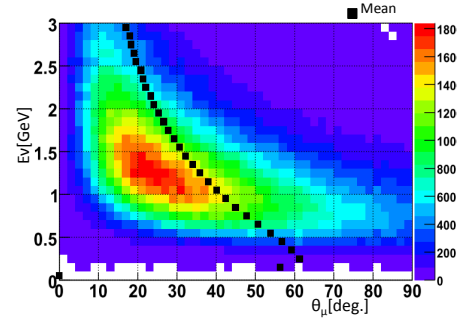


Figure 3.24: The neutrino energy VS. the muon angle generated from CC interactions. Black rectangle shows the mean energy at each angular bin.

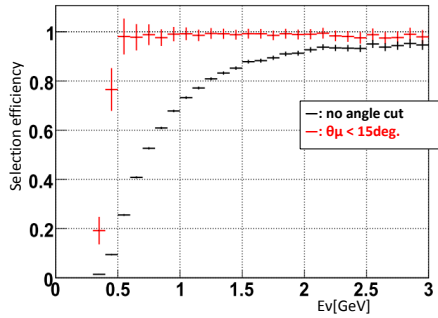


Figure 3.25: The selection efficiency for CC interactions for the muon with all angle and less than 15 degree

## Chapter 4

# Event rate measurements

### 4.1 Data set

We analyze the beam data from January to June, 2010. Data taking period, number of good spills and number of INGRID good spills are summarized in Tab.4.1. Data taking efficiency for entire period is 99.9%, and total number of protons recorded at INGRID is  $3.255 \times 10^{19}$ . The MC simulation corresponds to an equivalent of  $100 \times 10^{21}$  pot.

### 4.2 Event rate stability

We measured the event rate of the neutrino event candidates and the beam related dirt muon candidates with all fourteen modules. Here the dirt muon candidate is defined as the event rejected at upstream VETO selection or the fiducial volume cut. Figure 4.1 and Fig.4.2 show the daily pot and number of the neutrino event candidates, and number of dirt muon candidates, respectively. Figure 4.3 and Fig.4.4 show daily event rate normalized by pot. We succeeded to measure the daily event rate of neutrino event candidate and dirt muon

MR run #	Period	Good spills	INGRID good spills	Protons at CT05
29	Jan. 23 - Feb. 5	26813	26813	$0.32 \times 10^{18}$
30	Feb. 24 - Feb. 28	59256	59070	$1.12 \times 10^{18}$
31	Mar. 19 - Mar. 25	86980	86935	$1.97 \times 10^{18}$
32	Apr. 14 - May. 1	237350	236647	$7.64 \times 10^{18}$
33	May. 9 - Jun. 1	350079	350012	$1.22 \times 10^{19}$
34	Jun. 7 - Jun. 26	246504	246410	$9.30 \times 10^{18}$
Total		1006982	1005887	$3.26 \times 10^{19}$

Table 4.1: Summary of data sets

226 candidate with about 1.7% and 1.1% statistical error each day. The chi-squares  
 227 calculated from the average rate are 86 and 82 for 76 degrees of freedom. It is  
 228 concluded that the beam events is stable within statistical error.

## 229 4.3 The data/MC ratio

230 To obtain the number of events in the fiducial volume, we need to do following  
 231 corrections.

### 232 (1) Iron mass

233 In INGRID most of the neutrino interactions occur in the 9 iron targets  
 234 of each module. During their fabrication, there was a tolerance on the  
 235 thickness of those iron planes. This results in iron planes having slightly  
 236 different volumes, and as a consequence different masses. The maximal  
 237 variation from design mass is 2.15 % from the given tolerance on thickness.  
 238 The mass of each iron plane was measured at the end of the fabrication  
 239 process, so we can deduce correction factors for the expected number of  
 240 events for each module, by using the fact that 95.2 % of interactions in  
 241 one module occur in the iron.

### 242 (2) Accidental MPPC noise

243 Another correction on the number of observed events comes from noise  
 244 hits in the detector. Those noise hits reduce the number of reconstructed  
 245 events compared to the case when there is no noise. To correct this effect,  
 246 we use the following procedure:

- 247 · Measure noise in data
- 248 · Create a noise simulation to reproduce those measurements
- 249 · Use Monte Carlo simulation to compare the number of reconstructed  
 250 events with and without adding noise
- 251 · Deduce from the simulation correction factors and systematic errors

252 Noise is measured in beam data. We measure the rate of noise hits, which  
 253 are defined as hits occuring in the detector when no particles are actually  
 254 going through the detector. To find such hits, we look at cycles where  
 255 beam spills are not coming (INGRID records data on 23 integration cycles,  
 256 but beam spills only arrive during 6 of them), and perform regular event  
 257 selection to make sure there is no cosmic particle in the detector. We then  
 258 measure a noise rate for each channel of the detector, as well as light yield  
 259 and timing distribution.

260 Noise is then simulated with a given probability for each channel. Timing  
 261 for the noise hits is simulated using the distribution measured in data.  
 262 Light yield is then simulated using a measured light yield distribution for  
 263 the corresponding timing.

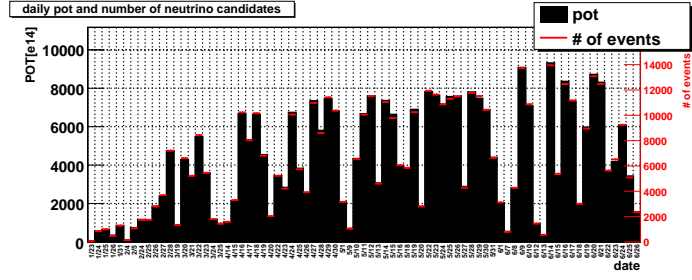


Figure 4.1: daily pot and number of neutrino event candidates

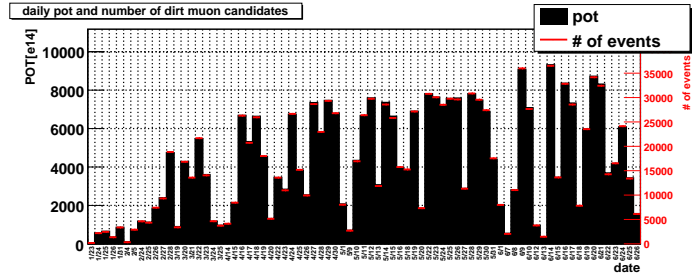


Figure 4.2: daily pot and number of dirt muon candidates

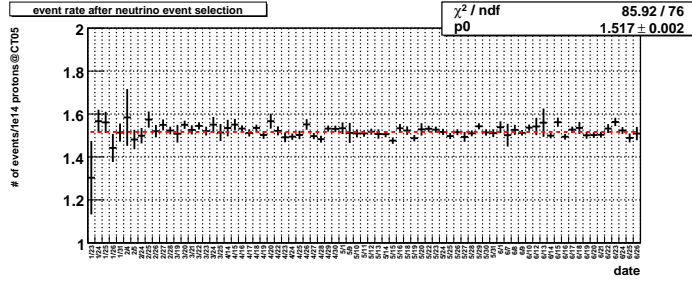


Figure 4.3: daily event rate of neutrino event candidate

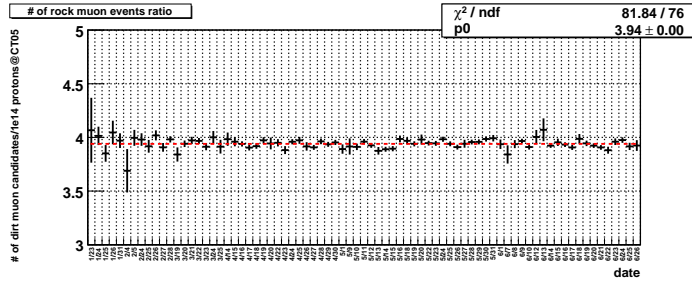


Figure 4.4: daily event rate of dirt muon candidate

Monte Carlo simulation is then used to measure the variation of number of reconstructed events due to noise. We first reconstruct events on Monte Carlo files which do not include noise hits, then add noise hits to those files and perform reconstruction again. We then compare the number of reconstructed events in each case. The simulation is using jnubeam 10c.

From this simulation we have for each module a noise rate and the variation of number of reconstructed events due to noise. There is a linear relation between them as can be seen on Fig.4.5. We will use this linear relation to make corrections on the number of observed events. This relation is:

$$\text{Variation of number of events } [\%] = -0.9585 * < \text{noise rate} >$$

Those corrections are made for each module, and each subset of events we are considering. In each case we measure the noise rate, and then from the linear relation deduce the variation of number of reconstructed events which should be used as a correction factor.

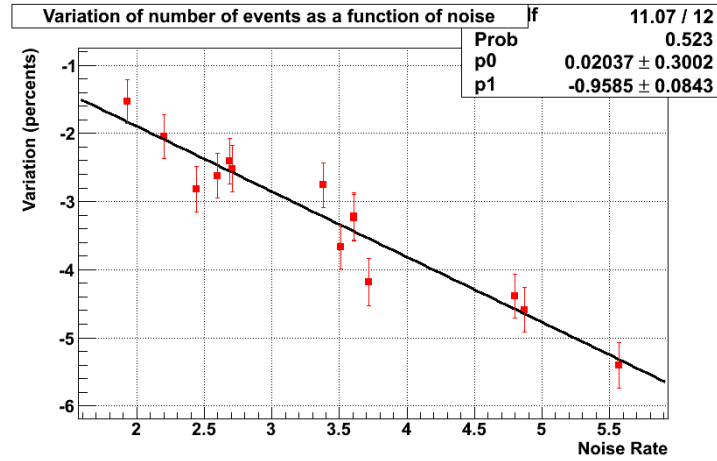


Figure 4.5: Variation of number of reconstructed events as a function of noise rate

### (3) Beam related background

We estimated the contamination fraction of beam related background with background MC in which the neutrino flux and the neutrino interaction is generated in upstream dirt (  $10 \times 10 \times 5 \text{ m}^3$  ).

Almost all contaminations come from short track induced neutron ( $\sim 50\%$ ) or gamma ( $\sim 40\%$ ) and dirt muon ( $\sim 10\%$ ) which is not detected accidentally due to scintillator inefficiency.



286 In background MC, number of generated interactions is normalized so that  
 287 the number of rejected events at upstream VETO selection, which consists  
 288 dirt muon mainly, is equal to DATA. The difference from POT expectation  
 289 is 35% and it is considered as systematic error. Finally contamination  
 290 fraction is estimated to be 0.4% and it is applied as one of the correction  
 291 factor.

292 The correction factors are summarized in Tab.4.2 run by run and module by  
 293 module. In this table the corrected number of selected events ( $N^{\text{cor.}}$ ) is calcu-  
 294 lated with  $N^{\text{cor.}} = N^{\text{sel.}} \times \frac{1}{1+C}$ , where  $N^{\text{sel.}}$  is the number of selected events and  
 295 C is the correction factor. The final result is summarized in Table 4.3. Finally  
 296 we obtain DATA/MC to be  $1.074 \pm 0.001$  (stat.).

	module	29,30	31	32	33	33	34
number of selected events	0	1054	1548	5956	4119	5425	6962
	1	1526	2033	7827	5432	7122	9520
	2	1875	2476	9360	6492	8555	11622
	3	1882	2570	10133	6795	9078	12191
	4	1831	2459	9627	6636	8683	11651
	5	1524	2176	7876	5421	7217	9588
	6	1058	1585	5837	4172	5421	7285
	7	1229	1717	6636	4509	5826	8100
	8	1588	2187	8351	5819	7620	10270
	9	1884	2562	9770	6632	8766	11946
	10	1949	2681	10305	6987	9373	12473
	11	1908	2520	9771	6713	8897	11871
	12	1561	2133	8146	5512	7193	9822
	13	1218	1659	6263	4327	5815	7734
correction factor	0	-3.3	-3.3	-4.3	-4.0	-3.9	-3.9
	1	-2.6	-2.6	-2.6	-2.4	-2.4	-2.4
	2	-2.0	-2.0	-2.0	-1.7	-1.7	-1.7
	3	-2.3	-2.3	-2.3	-2.0	-1.9	-1.9
	4	-1.8	-1.8	-1.8	-1.6	-1.5	-1.5
	5	-1.9	-1.9	-1.9	-1.6	-1.5	-1.4
	6	-2.3	-2.3	-2.8	-2.5	-2.4	-2.3
	7	-2.7	-2.7	-2.5	-3.5	-3.3	-3.1
	8	-2.2	-2.2	-2.0	-3.0	-2.8	-2.6
	9	-2.1	-2.1	-2.7	-4.1	-3.8	-3.6
	10	-4.2	-4.2	-4.1	-5.4	-5.2	-5.0
	11	-1.9	-1.9	-1.8	-2.9	-2.7	-2.6
	12	-4.9	-4.9	-4.7	-6.2	-6.0	-5.9
	13	-2.5	-2.5	-2.5	-3.4	-3.2	-3.0
corrected number of selected events	0	1090	1601	6224	4292	5647	7242
	1	1567	2087	8037	5565	7298	9756
	2	1913	2526	9551	6606	8703	11822
	3	1927	2632	10374	6934	9255	12422
	4	1865	2504	9804	6741	8817	11825
	5	1553	2218	8028	5509	7328	9697
	6	1083	1622	6002	4278	5552	7453
	7	1263	1765	6803	4674	6024	8360
	8	1624	2237	8520	6001	7838	10545
	9	1925	2617	10040	6912	9110	12391
	10	2035	2800	10742	7385	9883	13130
	11	1945	2569	9951	6914	9143	12183
	12	1641	2242	8550	5878	7653	10435
	13	1250	1702	6421	4478	6005	7976

Table 4.2: Correction factors

Number of selected events	493813
Corrected number of events	508511
Number of selected events in MC	4.733e5

Table 4.3: Number of events before and after corrections

## 4.4 Systematic error of event rate

Table 4.4 shows the systematic errors.

Item	Error[%]
Iron mass	0.1
Accidental MPPC noise	0.7
Beam related background	0.2
Fiducial selection	1.1
Hit efficiency	1.8
Tracking efficiency	1.4
Track matching selection	2.7
Not beam-related background	<0.1
p.e./active layer selection	<0.1
Beam timing selection	<0.1
Total	3.7

Table 4.4: Systematic error table

298

### Iron mass

Before construction of INGRID the mass of each iron plate was measured with a precision of 1 kg, which corresponds to 0.13 % of the mass of one iron plate. We will use this figure as the systematic error on this correction factor. We might need to increase this systematic error in the future, as the correction factors are calculated using the mass of the whole iron plate, when we actually use a fiducial cut in analysis, only interactions in the central part of the iron plates are kept.

### Accidental MPPC noise

The effect of MPPC noise is studied with MC as discussed at previous chapter. Two sources of systematic errors are considered. First one comes from the error on the linear fit. To get this systematic error, we multiply the fit error by the maximal measured noise rate. Second one comes from the measurement of noise. Correction factors are calculated using the average noise rate measured on one period. But this noise rate fluctuates in time (probably due to temperature variations). So we measure the maximal difference between average noise rate

and noise rate measured at different times during one period, and using the linear relation between noise rate and variation of number of events we get the systematic error. The quadratic sum of these two errors is 0.7 %.

### Beam-related background

We estimated the contamination fraction of beam related background with wall neutrino Monte Carlo. The fraction is estimated to be 0.4% , in which the number of interactions of background is normalized to compare the number of dirt muon in DATA and MC. There is a 35% difference from POT expectation, which is considered as one of the source of the systematic error. We considered 20% neutrino flux uncertainty and 20% cross section uncertainty as other sources of the systematic error. Finally 0.2% ( $=\sqrt{0.35^2 + 0.2^2 + 0.2^2}$ ) is applied as the systematic error.

### Fiducial selection

To estimate the uncertainty of fiducial selection and the effect of non uniformity of iron plate, we divided fiducial in several horizontal slices and checked the difference between DATA and MC. Table 4.5 shows the result. The maximum absolute value, 1.1%, is applied as systematic error.

selection	DATA	MC	DATA - MC
<50 cm from center(nominal selection)	100.0	100.0	0.0
<25 cm	25.6	25.2	0.4
25 ~ 40 cm	39.9	39.3	0.6
40 ~ 50 cm	34.4	35.5	1.1
Systematic error ( Maximum absolute )			1.1

Table 4.5: DATA-MC for several sub fiducial volume

### Hit efficiency

We estimated the relation between hit efficiency and number of selected events with MC. Fig. 4.6 shows the result from which the systematic error of hit efficiency is estimated to be 1.8% because hit efficiency has 1.1% uncertainty. <sup>1</sup>

### Track matching selection

In the neutrino event selection, after reconstruction of XZ track and YZ track we require track start point matching. To estimate the uncertainty of the selection, we changed the tolerance for the matching and checked the difference of the

<sup>1</sup>0.5% of the measurement error of hit efficiency, 1.0% of the tuning of hit efficiency in MC

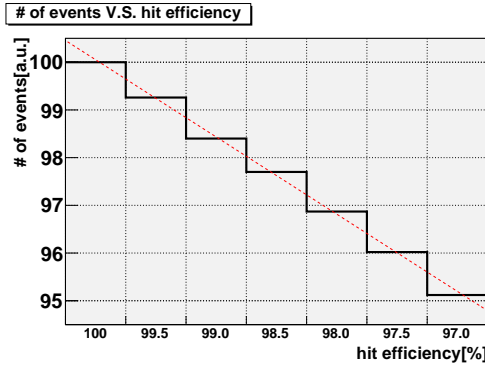


Figure 4.6: hit efficiency V.S. number of selected events

number of selected events between DATA and MC. Table 4.6 shows the result. The maximum absolute value, 2.7%, is applied as systematic error.

Vertex Z of XZ track - Vertex Z of YZ track	DATA	MC	DATA - MC
-1, 0, +1 (nominal selection)	100.0	100.0	0.0
0	83.0	85.7	2.7
-2, -1, 0, +1, +2	104.0	103.0	1.0
Systematic error ( Maximum )			2.7

Table 4.6: DATA-MC for several tolerance of track matching.

342

### 343 Tracking efficiency

344 To check the difference of the tracking efficiency between DATA and MC, the  
345 tracking efficiency is compared with several sub-sample selected by number of  
346 active planes. Table 4.7 shows the result. The maximum absolute value, 1.4%,  
347 is applied as systematic error.

### 348 Not beam-related background

349 The off-bunch data (cycle 17 ~ 22 where as on-bunch cycle is 4 ~ 9) are analyzed  
350 with same procedure and only 93 events are selected whereas the number of  
351 signal is 493813. It is negligible.

### 352 PE/active layer selection

353 To estimate the uncertainty of PE/active layer selection, we changed the cut  
354 value and checked the difference of number of selected events from one with

number of active planes	DATA	MC	DATA - MC
3	87.6	86.9	0.7
4	93.2	91.8	1.4
5	94.7	94.3	0.5
6	95.6	96.2	0.6
7	96.2	96.6	0.4
8	96.7	96.8	0.1
9	98.7	97.9	0.8
10	99.1	99.0	0.1
Systematic error ( Maximum )			1.4

Table 4.7: The tracking efficiency of DATA and MC with several sub sample

nominal cut. The result is the difference is less than 0.01% and its uncertainty is negligible.

#### beam timing selection

To estimate the uncertainty from neutrino beam timing, we changed the cut value and checked the difference of number of events from nominal cut. The difference is less than 0.01% and it is negligible.

## Chapter 5

# Measurements of beam profile

We measured the beam profile on a monthly basis, which corresponds to MR run number. Fig.5.1 shows horizontal and vertical beam profile with RUN 32 data. We fit the profile with gaussian function with least square method and fitted center and sigma are applied as beam center and beam width, respectively.

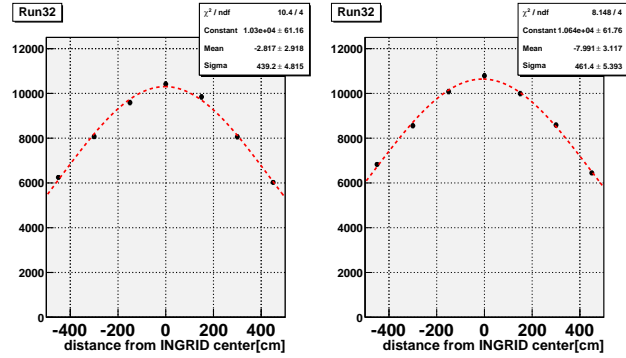


Figure 5.1: Horizontal profile(left) and vertical profile(right)

### 5.1 Stability of beam center

Figure 5.4 shows the monthly x center and Fig.5.5 show the monthly beam y center. We succeeded to measure the profile center with about 4.2 cm statistical error for each month. The chi-square calculated from the average rate are 4.1 for 5 degrees of freedom for x beam centers and 3.8 for 5 degrees of freedom for

373 y beam centers. It is concluded that the beam center is stable within statistical  
 374 error.

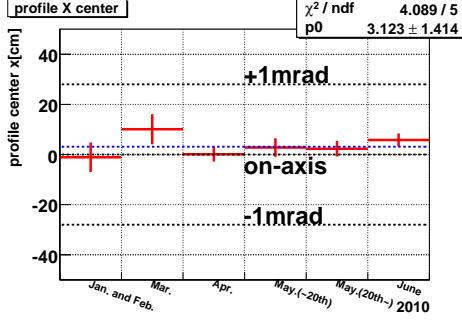


Figure 5.2: Horizontal profile center.

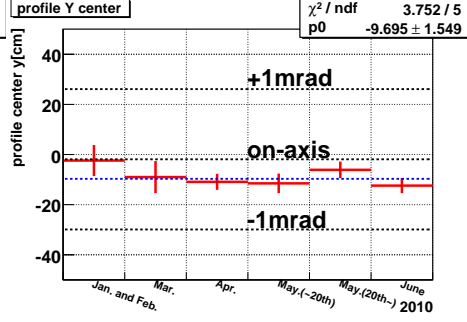


Figure 5.3: Vertical profile center

## 375 5.2 The systematic error of beam center

376 We estimated the systematic error using the toy profile MC simulation in which  
 377 the number of events at each module is varied with 3.7% from original profile  
 378 made by all the beam data. 100'000 profiles are generated and the beam center  
 379 is measured with same method as the data analysis. Figure 5.4 and Fig.5.5 show  
 380 the x center distribution and y center distribution, respectively. The RMS is  
 381 applied as the systematic error. The result shows 9.2 cm for x center and 10.4  
 382 cm for y center.

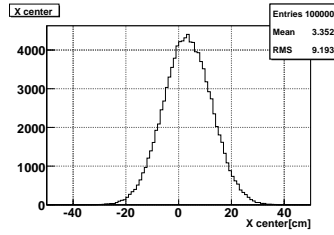


Figure 5.4: Fitted Horizontal center  
with 100'000 profiles

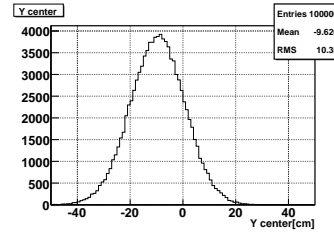


Figure 5.5: Fitted Vertical center with  
100'000 profiles



## Chapter 6

# Measurement of beam direction

The beam direction is measured as a direction from the proton beam target to the beam center measurements summarized in Tab.6.1. Table 6.2 shows the result of survey of the positions of proton beam target, the center of INGRID horizontal modules and vertical modules (based on the result put on [4]). With these measurements we calculate the beam direction and result is shown in Tab. 6.3; Depression angle is  $3.651 \pm 0.0216$  degrees and direction angle is  $270.475 \pm 0.0190$ . Table 6.3 shows also the result of survey of the angle between the target and the SK detector. Finally the off-axis angle is obtained to be  $2.519 \pm 0.021$  degrees ( $43.96 \pm 0.37$  mrad).

Table 6.1: Summary of beam center measurements

	X center	Y center
Measurement	$+0.2 \pm 9.3$	$-6.6 \pm 10.5$

Table 6.2: The position with the NEUT coordinate system

	X[m]	Y[m]	Z[m]
Target	0	0.30603	-4.62
INGRID H center	-0.000863	-17.55557	277.36844
INGRID V center	-0.038371	-17.38257	273.35956

Table 6.3: Direction from the proton beam target and SK

	Depression[degree]	Direction[degree]	Angle from SK[degree]
SK	1.260	270.475	-
INGRID center	3.637	269.681	2.506
	3.651	270.475	$2.519 \pm 0.0213$
INGRID measurement	$\pm 0.0216$	$\pm 0.0190$	$(43.96 \pm 0.37 \text{ mrad})$

## Chapter 7

## Conclusion

In this note we have presented the measurement of the neutrino event rate, profile center in INGRID during and beam direction with 2010a data. We selected the neutrino interactions to reconstruct the long track started within fiducial volume. The results have been compared to MC and found good agreement with DATA. Finally DATA/MC of the event rate and beam profile centers have been evaluated with an associated systematic error:

$$\begin{aligned} R_{\text{DATA/MC}} &= 1.074 \pm 0.001(\text{stat.}) \pm 0.040(\text{syst.}) \\ X_{\text{center}} &= +0.2 \pm 1.4(\text{stat}) \pm 9.2(\text{syst.})\text{cm} \\ Y_{\text{center}} &= -6.6 \pm 1.5(\text{stat.}) \pm 10.4(\text{syst})\text{cm} \\ \text{offaxis angle} &= 2.519 \pm 0.021\text{degrees} \\ &= 43.96 \pm 0.37\text{mrad} \end{aligned}$$

## 403 Bibliography

404 [1] will be put the name of jnubeam tech. note

405 [2] will be put the name of NEUT doc.

406 [3] the report by Calibration group of ND280 working group put  
407 on [http://www.t2k.org/nd280/calib/Meetings/Jan10Workshop/](http://www.t2k.org/nd280/calib/Meetings/Jan10Workshop/MPPClinearity/at_download/filet2k.org)  
408 [MPPClinearity/at\\_download/filet2k.org](http://www.t2k.org/nd280/calib/Meetings/Jan10Workshop/MPPClinearity/at_download/filet2k.org)).

409 [4] <http://www.t2k.org/beam/NuFlux/GeometryInformation>